Microchimica Acta
https://doi.org/10.1007/s00604-018-3129-3

ORIGINAL PAPER

A phenylboronate-based SERS nanoprobe for detection and imaging of intracellular peroxynitrite

Hua-Ying Chen[1] · Dan Guo[1] · Zhen-Fei Gan[1] · Lei Jiang[1] · Shuai Chang[1] · Da-Wei Li[1]

Received: 8 August 2018 / Accepted: 29 November 2018

Abstract

A surface-enhanced Raman scattering (SERS) based nanoprobe was developed for detection and imaging of endogenous peroxynitrite in living cells. The probe was fabricated by assembling 3-mercaptophenylboronic acid pinacol ester onto the surface of gold nanoparticles (AuNPs). The detection of peroxynitrite is accomplished via measurement of the changes in the SERS spectra (at 882 cm^{-1}) that are caused by the reaction between probe and peroxynitrite. The probe has a fast response (<30 s), a 0.4 μM lower detection limit and a wide linearity range from 5.0×10^{-7} to 1.0×10^{-4} M. It is biocompatible and highly stable on storage and under various pH conditions. Both the reaction and the SERS signal are highly specific over other species. The nanoprobe was successfully applied to SERS imaging of peroxynitrite that is produced in macrophages under oxidative stress. Conceivably, the method has a most viable tool for use in studies on peroxynitrite-related physiological and pathological processes.

Keywords Gold nanoparticles · Boronate ester · Biosensor · Specific reaction · Surface-enhanced Raman scattering · Reactive oxygen species · Oxidative stress · Living cell

Introduction

Peroxynitrite ($ONOO^-$) is a reactive oxygen species that is strongly related to diverse physiological processes [1, 2]. The aberrant concentration of $ONOO^-$ is closely involved into various disorders, such as neurodegenerative diseases, traumatic brain injury and inflammatory diseases [3–5]. Therefore, it is of great significance to detect $ONOO^-$ in biological system for deeply understanding its pathological functions. Currently, there are a number of methods for the detection of $ONOO^-$, such as electrochemical and fluorescent approaches [6, 7]. Electrochemical processes have fast response and high sensitivity, but their applications in cell tests are usually complicated due to the implanting ways of the sensors [7]. Fluorescent methods allow detection and imaging for living cells, whereas it is difficult to keep the stability of fluorescent probes in the measurement medium owing to photo- and chemical bleaching [7, 8]. Moreover, fluorescent methods can hardly avoid phototoxicity and the background interference of biological samples whose proteins, coenzymes and pigments often exhibit intrinsic fluorescence [7–9].

SERS has increasingly emerged as a powerful analytical technology which not only provides fingerprint spectra of analytes but also possesses high sensitivity and chemical specificity [10, 11]. Owing to these advantages of SERS, it has been widely applied in biological analysis [12, 13]. For instance, DNA has already been detected by silver nanoparticles modified with spermine molecules or iodide to obtain sensitive SERS signals of DNA [14–16]. And proteins have been analyzed by SERS method with improved recordable compact disks as SERS substrates [17]. Nevertheless, there still remains one trouble for SERS method to measure biologically inorganic small molecules because of their poor SERS responsiveness resulting from narrow Raman cross section [18]. Through integrating SERS-active nanostructures with Raman reporter molecules which are also able to react with analytes, nanoprobes can be constructed to overcome that trouble and take full advantage of SERS [10]. In this way, biologically inorganic small molecules such as nitric oxide and hydrogen peroxide have successfully been achieved

Electronic supplementary material The online version of this article (https://doi.org/10.1007/s00604-018-3129-3) contains supplementary material, which is available to authorized users.

✉ Da-Wei Li
daweili@ecust.edu.cn

[1] Key Laboratory for Advanced Materials, Shanghai Key Laboratory of Functional Materials Chemistry, School of Chemistry and Molecular Engineering, East China University of Science and Technology, 130 Meilong Road, Shanghai 200237, China

Published online: 10 December 2018

according to the changes of SERS spectra of the nanoprobes [10, 19]. However, to the best of our knowledge, this type of reaction-based SERS nanoprobe for the highly selective and sensitive in-situ analysis of the endogenous $ONOO^-$ in living cells has not been reported yet.

Herein, inspired by the mechanism that aromatic boronate derivatives can react with $ONOO^-$ specifically [20], we developed a novel SERS nanoprobe. As displayed in Fig. 1, the nanoprobe was fabricated by modifying newly synthesized 3-mercaptophenyl boronic acid pinacol ester (3-MPBAPE) onto the surface of gold nanoparticles (AuNPs). In the presence of $ONOO^-$, the boronate moiety of 3-MPBAPE is turned into hydroxyl group, resulting in distinct changes in SERS spectrum of the AuNP/3-MPBAPE nanoprobe. Based on these SERS changes, the detection of $ONOO^-$ can be achieved with high selectivity and sensitivity. Furthermore, the in-situ detection and visualized tracking of endogenous $ONOO^-$ in living cells can be accomplished by using this kind of SERS nanoprobe.

Experimental section

Materials and reagents

Hydrogen tetrachloroaurate trihydrate ($HAuCl_4 \cdot 3H_2O$, 99%), trisodium citrate trihydrate ($C_6H_5Na_3O_7 \cdot 3H_2O$, ≥99.8%) were obtained from Energy Chemical (Shanghai, China, https://www.energy-chemical.com/). $ONOO^-$ reagent was purchased from Cayman Chemical Company (USA, http://www.caymanchem.com). Lipopolysaccharides (LPS), interferon-γ (IFN-γ), phorbol 12-myristate 13-acetate (PMA), sodium hypochlorite (NaClO, ≥99.7%), diethylamine NONOate sodium salt hydrate (≥97%), ascorbic acid (AA, ≥99%), RPMI-1640 medium and fetal bovine serum (FBS) were acquired from Sigma-Aldrich Inc. (USA, https://www.sigmaaldrich.com). Hydrogen peroxide (H_2O_2, 30 wt.%), sodium chloride (NaCl, ≥99.7%), iron protochloride ($FeCl_2$, 99.0%), copper chloride ($CuCl_2$, 99.0%), sodium nitrate ($NaNO_3$, 99.0%), sodium nitrite ($NaNO_2$, 99.0%) and 3-mercaptophenol (3-MP, 96%) were bought from Aladdin-Reagent Co., Ltd. (Shanghai, China, http://www.aladdin-e.com/). Murine macrophage cell line RAW264.7 was purchased from American Type Culture Collection (Manassas, VA, USA, https://www.atcc.org/). All experimental solutions were prepared by deionized water (18 MΩ·cm, Millipore) and chemicals were used in the experiments without further purification.

Apparatus

The morphology characterization of nanoprobes was performed by transmission electron microscope (TEM, JEM-2100, JEOL, Japan). The distribution of nanoprobes was measured by UV–Vis spectroscopy (Agilent Technologies Cary 60, USA). The molecular information of the newly synthesized 3-MPBAPE was analyzed by nuclear magnetic resonance (NMR) spectrometer (AVANCEIII, Switzerland) and mass spectrometer (GCT Premier, Waters, USA). The bright-field and dark-field images of the RAW264.7 cells incubated with AuNP/3-MPBAPE nanoprobe were captured by an inverted microscope (Eclipse Ti-U, Nikon, Japan) equipped with a dark-field condenser ($0.8 < NA < 0.95$), a 100 W halogen lamp, a true-colour CCD camera, and a × 40 objective lens (NA = 0.6). SERS spectra and

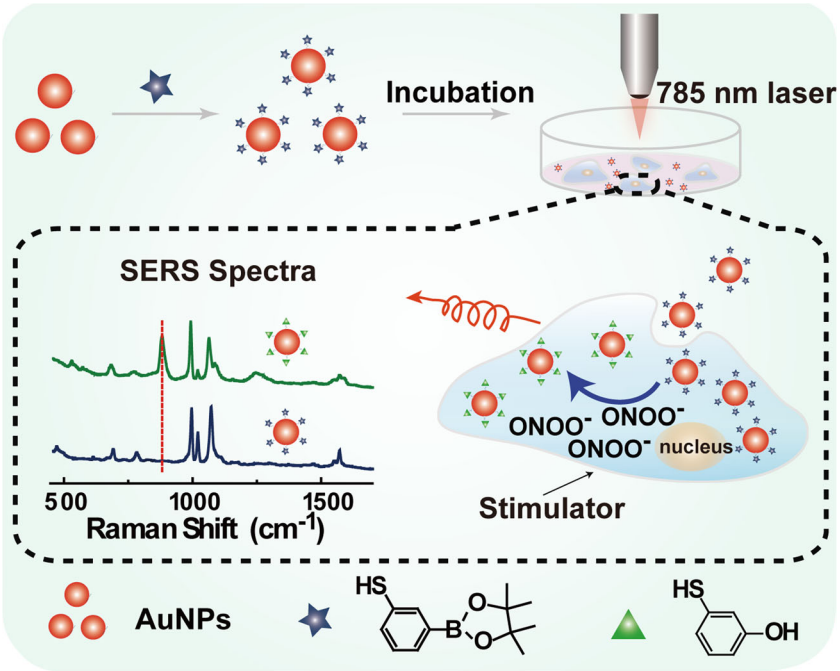

Fig. 1 Schematic illustration of the detection of endogenous $ONOO^-$ in living cells with AuNP/3-MPBAPE nanoprobe

SERS mapping were collected by a confocal Raman microscope (JY LabRAM XploRA PLUS, Horiba, Japan). The laser excitation wavelength used was 785 nm with a power of 9 mW at the sample. The scan over a single cell was carried out on a computer-controlled XY stage in 2 μm steps and with 2 s as the integration time per step.

Synthesis of 3-mercaptophenylboronic acid pinacol ester (3-MPBAPE)

3-MPBAPE was newly synthesized as follows. Briefly, 3-bromothiophenol (0.945 g, 5 mmol) was dissolved in dry THF solvent under N_2 atmosphere. Then sodium hydride (0.180 g, 7.5 mmol) was slowly added and stirred for 1 h at −78 °C followed by addition of tert-butyldimethylsilyl chloride and further stirring for 24 h at room temperature. The mixed solution was extracted with ethyl acetate (EA) then were concentrated and purified to obtain intermediate **1**. A solution of intermediate **1** (0.604 g, 2.0 mmol) in DMF was mixed with bis(pinacolato)diboron (0.609 g, 2.4 mmol), [1,1'-bis(diphenylphosphino)ferrocene] dichloropalladium (II) (0.293 g, 0.4 mmol) and Cs_2CO_3 (1.629 g, 5.0 mmol) under N_2 atmosphere. After stirring at 80 °C for 12 h, the reaction mixture was poured into water and extracted with EA to obtain intermediate **2** after purification. Afterwards, trifluoroacetic acid (1.140 g, 10 mmol) was added into the solution of intermediate **2** in dichloromethane, which was agitated at ambient temperature and monitored with thin-layer chromatography. Thus, the ultimate product of 3-MPBAPE was acquired with chromatography purification (Scheme 1).

Fabrication of the nanoprobe

To fabricate the AuNP/3-MPBAPE nanoprobe, AuNPs were firstly synthesized according to the modified method of Lee and Meisel [21] (Synthesis of gold nanoparticles, ESM). The freshly prepared solution of 3-MPBAPE were mixed with the above AuNPs to achieve the assembling of 3-MPBAPE on the surfaced of AuNPs. Finally, the AuNP/3-MPBAPE nanoprobe was obtained after centrifuging and resuspending in phosphate buffered saline (20 mM; pH = 7.4) to remove the excess 3-MPBAPE molecules.

Solution tests

$ONOO^-$ was acquired in form of solution in NaOH (0.3 M) and stored at −80 °C. Before each usage, the $ONOO^-$ reagent was immediately thawed, and its concentration was determined with the absorbance measurement of the solution at 302 nm as the reported method [22]. Different amount of $ONOO^-$ was added into 200 μL freshly fabricated AuNP/3-MPBAPE nanoprobe solution, then SERS spectra of the nanoprobe were measured. To investigate the response selectivity of the AuNP/3-MPBAPE nanoprobe, diverse biologically relevant species at a certain concentration were respectively added into 200 μL nanoprobe solution, followed by the collection of SERS spectra. In addition, hydroxyl radical (•OH) was prepared with the Fenton reaction (Fe^{2+}/H_2O_2 = 10 μM: 60 μM) according to the previously described procedure [23]. Superoxide ($O_2^{\bullet-}$) was produced by adding xanthine in 1.6 M NaOH into xanthine oxidase solution with the following stirring at 25 °C for 1 h [24].

Cell tests

RAW264.7 cells were cultured overnight in RPMI-1640 medium supplemented with 10% fetal bovine serum (FBS), 100 μg·mL^{-1} penicillin, and 100 μg·mL^{-1} streptomycin at 37 °C in a 5% CO_2 incubator. To prepare cell samples for SERS detection and imaging, the cells were seeded in a quartz culture dish (ϕ 60 mm) with about 6×10^5 cells for one night to allow adherence. Then, the cells were treated with LPS and IFN-γ for 12 h followed by PMA for 2 h to stimulate endogenous $ONOO^-$. Three series of stimulation treatments were performed respectively using (1) 1 μg·mL^{-1} LPS, 50 ng·mL^{-1} IFN-γ and 0.06 μg·mL^{-1} PMA; (2) 4 μg·mL^{-1} LPS, 200 ng·mL^{-1} and 0.24 μg·mL^{-1} PMA; (3) 10 μg·mL^{-1} LPS, 500 ng·mL^{-1} IFN-γ and 0.6 μg·mL^{-1} PMA. The cell sample after a stimulation treatment was subsequently incubated with the culture media containing AuNP/3-MPBAPE nanoprobes for 2 h at 37 °C. After washing with buffer (pH = 7.4) three times to remove remnant nanoprobes unbound cells, the culture dish was mounted to on the microscope stage to perform imaging and spectroscopic detection.

Results and discussion

Characterization of AuNP/3-MPBAPE nanoprobe

The 3-MPBAPE molecule with a mercapto group for forcefully bonding of 3-MPBAPE on AuNPs surface and a boronate moiety for specifically reacting with $ONOO^-$ was newly synthesized. And it was confirmed by 1H-NMR

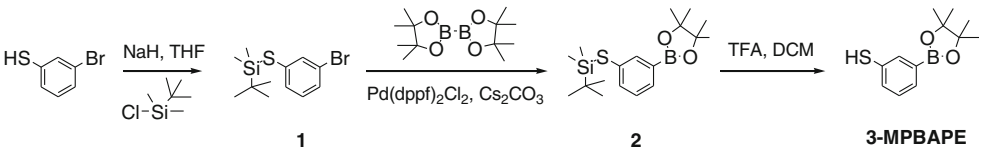

Scheme 1 Synthetic route of 3-MPBAPE

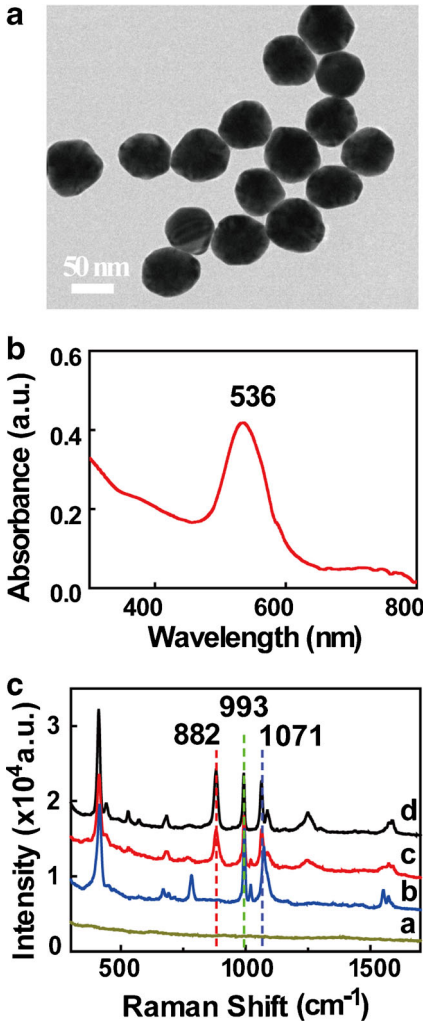

Fig. 2 **a** Typical TEM image of AuNP/3-MPBAPE nanoprobe, the scale bar represents 50 nm; **b** UV–Vis spectrum of AuNP/3-MPBAPE nanoprobe; **c** SERS spectra of (**a**) AuNPs, (**b**) AuNP/3-MPBAPE nanoprobe, (**c**) AuNP/3-MPBAPE nanoprobe reacting with $ONOO^-$, and (**d**) AuNP/3-MP

spectroscopy, 13C-NMR spectroscopy, and mass spectrometry shown in Fig. S1-S3. Through modifying 3-MPBAPE on the surface of AuNPs in virtue of the Au-S bond formed with ease, the nanoprobe was fabricated quickly and conveniently in solution. Morphology characterization by TEM demonstrates that the shape of the AuNP/3-MPBAPE nanoprobe is spherical and the size is about 60 nm (Fig. 2a). Furthermore, a narrow UV–Vis peak at 536 nm can be observed for the AuNP/3-MPBAPE solution (Fig. 2b). It indicates that the fabricated nanoprobe has good dispersity with particle size about 60 nm, agreeing well with the TEM result. Moreover, SERS measurement of the nanoprobe demonstrates that an obvious SERS spectrum can be observed after mixing 3-MPBAPE with AuNPs shortly (Fig. 2c-b). This means that 3-MPBAPE is successfully assembled on AuNPs since SERS is a surface-selective technique [25]. After addition of $ONOO^-$, a new peak appears at 882 cm^{-1} in the SERS spectrum of the nanoprobe (Fig. 2c-c), which can be clearly distinguished from the blank control (Fig. 2c-b). According to the theoretical calculation shown in Table S1, the peak at 882 cm^{-1} is caused by the stretching vibration of C-O combining with scissoring vibration of CCC ring. In addition, the peaks at 993 and 1071 cm^{-1} can be assigned to the CCC ring stretching and the CCC ring stretching with mixing of HCCH rocking vibration. More importantly, the profile of SERS spectrum of the nanoprobe after reacting with $ONOO^-$ (Fig. 2c-c) is well consistent with that of 3-MP (Fig. 2c-d). This further verifies that the boronate moiety of 3-MPBAPE is transformed into phenolic hydroxyl group.

The response speed of the AuNP/3-MPBAPE nanoprobe was explored by collecting SERS spectra with the addition of $ONOO^-$ (50 μM) for different time. As shown in Fig. 3, the intensity of SERS peak at 882 cm^{-1} (characteristic of $ONOO^-$) increases rapidly after $ONOO^-$ addition with peak at 993 cm^{-1} almost invariable, and the ratiometric peak intensity of I_{882}/I_{993} reaches a plateau after 30 s. The result implies that the nanoprobe can have rapid response to $ONOO^-$, which may be ascribed to the catalytical effect of AuNPs on the sensing reaction [26]. Therefore, the nanoprobe is capable of detecting the active and short-lived $ONOO^-$ in the biological media.

For a robust SERS nanoprobe, it is also important to remain stable in biological detections. Therefore, the temporal and pH stability of the nanoprobe was investigated, and the

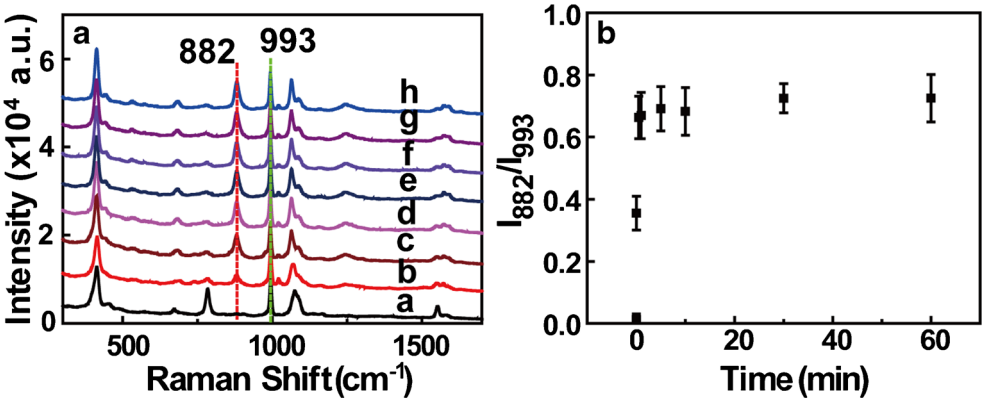

Fig. 3 **a** SERS response of AuNP/3-MPBAPE nanoprobe in phosphate buffered saline (pH = 7.4) after reacting with 50 μM $ONOO^-$ for different time (**a**–**h**): 0 s, 10 s, 30 s, 1 min, 5 min, 10 min, 30 min, and 60 min. **b** Plots of I_{882}/I_{993} versus reaction time. Each data point represents the average value calculated from three replicate SERS spectra

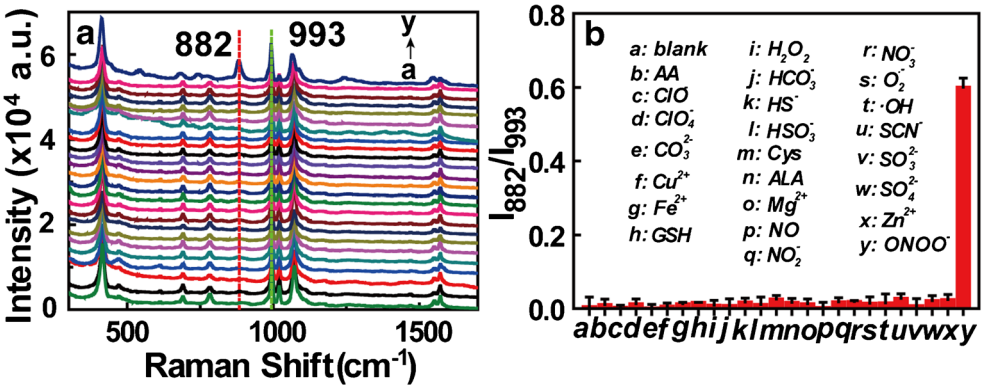

Fig. 4 Selectivity of AuNP/3-MPBAPE nanoprobe in buffer (pH = 7.4) in the presence of diverse biologically relevant species (c = 100 μM), [$ONOO^-$] = 20 μM. Each data point represents the average value calculated from three replicate SERS spectra

corresponding results are shown in Fig. S4 and S5. It can be seen that there is no obvious change in the ratiometric peak intensity when the nanoprobe is stored over 48 h and the pH value of solution changes from 5.4 to 9.7. This implies that the nanoprobe has good stability against time and pH, which means that the SERS nanoprobe is suitable for applications in intracellular detection. Moreover, the nanoprobe after reaction with $ONOO^-$ (AuNP/3-MP) can remain stable and resist the impact of pH condition of the tested solution (Fig. S6). These features are in favor of making the SERS signals in living cells more reliable.

Selectivity of the AuNP/3-MPBAPE nanoprobe

The selectivity of the nanoprobe was investigated by recording its SERS spectra in the separate presence of $ONOO^-$ and other relevantly biological species, such as glutathione (GSH), L-cysteine (Cys), ALA, AA, HS^-, HSO_3^-, SCN^-, SO_3^{2-}, SO_4^{2-}, HCO_3^-, CO_3^{2-}, NO, NO_2^-, NO_3^-, ClO^-, ClO_4^-, H_2O_2, •OH, $O_2^{\bullet-}$, Mg^{2+}, Fe^{2+}, Cu^{2+} and Zn^{2+}. As shown in Fig. 4, only $ONOO^-$ can trigger obvious SERS peaks at 882 cm^{-1}, whereas other relevantly biological species do not give rise to SERS signals at the same Raman shift. This may be attributed to combined effects of two main factors: the specificity of the $ONOO^-$-sensing reaction and the fingerprinting feature of the SERS technique. It is worth noting that, although HClO and H_2O_2 are also considered to be reactive with phenylboronic acid compounds [27], they do not influence the detection of $ONOO^-$ in this work. This may be because that the speeds of their reactions with 3-MPBAPE on the SERS nanoprobe are much slower than that speed of the reaction involved with $ONOO^-$. As shown in Fig. S7, ClO^- and H_2O_2 cannot induce SERS response of the SERS nanoprobe at 882 cm^{-1} after reaction for 6 h. However, this response can be significantly initiated by $ONOO^-$ with similar concentration within 30 s. Similar results can be observed for other potential interfering species such as glucose, other saccharides (trehalose, mannose, galactose), nucleosides (adenosine, cytidine, guanosine, inosine and uridine), dopamine, bovine serum albumin, and homocysteine (Fig. S8). This indicates that those species have no obvious interference on the detection of $ONOO^-$ although glucose, other saccharides, nucleosides and dopamine are reported to be able to bind boronic acids [28, 29]. One possible reason is that the interaction

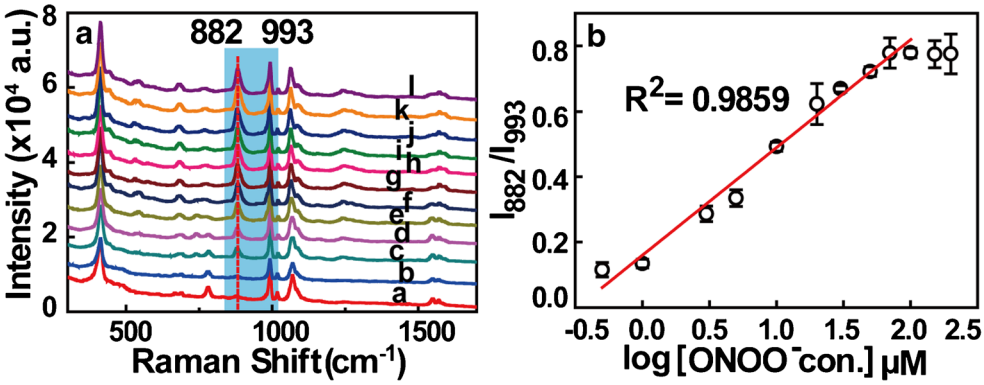

Fig. 5 **a** SERS spectra of AuNP/3-MPBAPE nanoprobe in buffer (pH = 7.4) in the presence of $ONOO^-$ with various concentrations (a-l): 0.5 μM, 1 μM, 3 μM, 5 μM, 10 μM, 20 μM, 30 μM, 50 μM, 70 μM, 100 μM, 150 μM and 200 μM. Bluish rectangle-marked range: 850 to 1010 cm^{-1}. **b** Plots of I_{882}/I_{993} versus the logarithmic concentration of $ONOO^-$. Each data point represents the average value calculated from three replicate SERS spectra

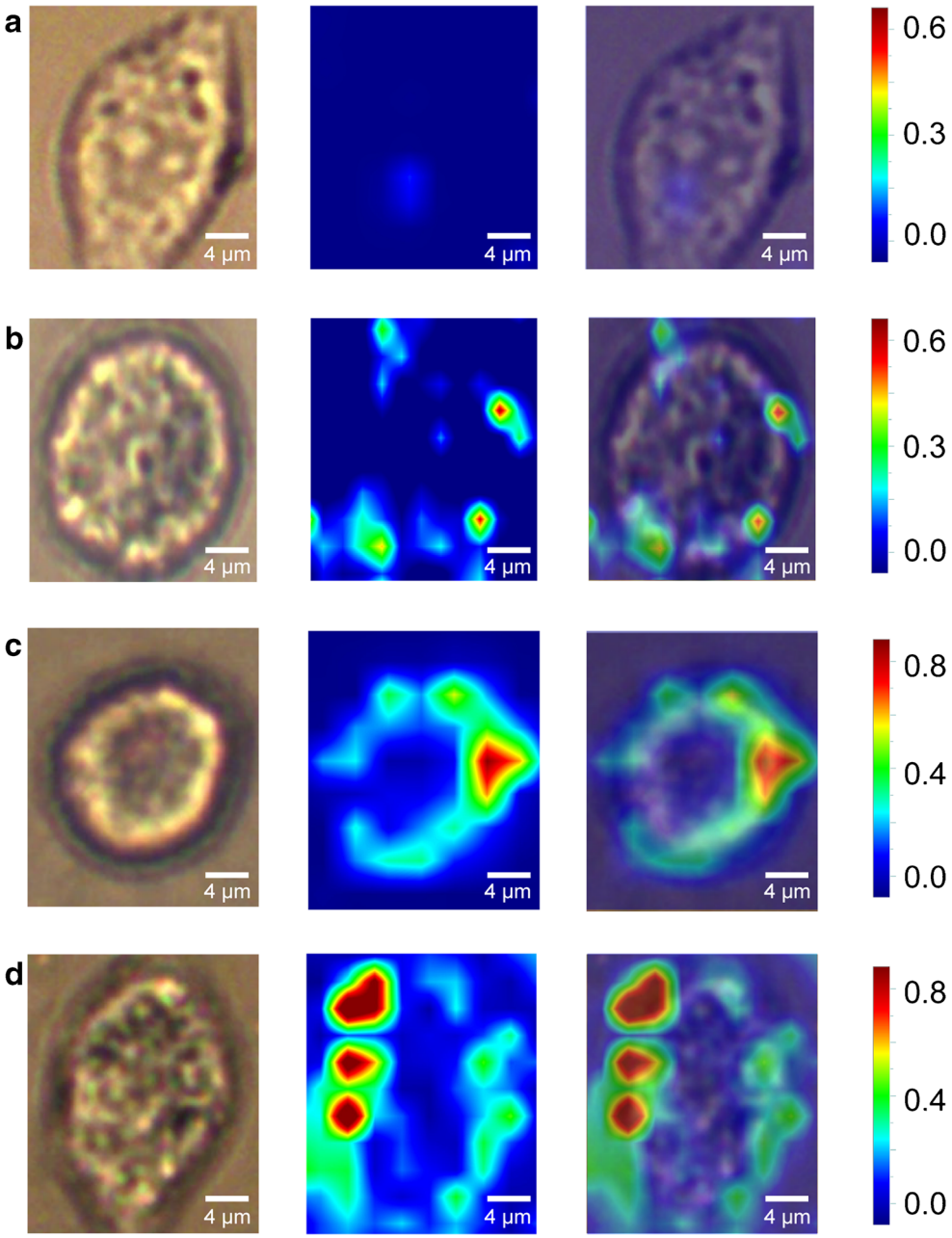

Fig. 6 SERS imaging of RAW264.7 macrophage cells treated with stimulants at different concentrations and then incubated with the AuNP/3-MPBAPE nanoprobe for 2 h (left: bright-field microscopy image; middle: SERS image; right: overlay image). **a** Control. **b** LPS (1 μg·mL^{-1}) and IFN-γ (50 ng·mL^{-1}) for 12 h, and PMA (0.06 μg·mL^{-1}) for 2 h. **c** LPS (4 μg·mL^{-1}) and IFN-γ (200 ng·mL^{-1}) for 12 h, and PMA (0.24 μg·mL^{-1}) for 2 h. **d** LPS (10 μg·mL^{-1}) and IFN-γ (500 ng·mL^{-1}) for 12 h, and PMA (0.6 μg·mL^{-1}) for 2 h

between 3-MPBAPE and those potential interferents is not as strong as that of boronic acids with above interferents. Even though some of those interferents bind to the phenylboronate ester, $ONOO^-$ can still overcome the protection given to the boron atom by the N-B interaction to avoid their interference [20]. Moreover, the thiol group of the synthesized 3-MPBAPE molecule is in favor of forcefully bonding to the surface of AuNPs to prevent from the interference of albumins and other thiols on the detection. This result further illustrates that the nanoprobe is able to detect the endogenous $ONOO^-$ in living cells without interference from other biological species.

Sensitivity of the AuNP/3-MPBAPE nanoprobe

The sensitivity of the nanoprobe was further evaluated in phosphate buffered saline (pH = 7.4) by measuring SERS signals in the presence of $ONOO^-$ with different concentrations. It can be seen from Fig. 5a that, as $ONOO^-$ concentration increasing, the SERS peak at 882 cm^{-1} related with the $ONOO^-$-sensing reaction is rising dependently. When the concentration of $ONOO^-$ is more than 100 μM, the ratiometric peak intensity of I_{882}/I_{993} gradually becomes steady. The result may be due to that all of the 3-MPBAPE molecules assembled on the nanoprobe are used up by

$ONOO^-$. Notably, the best Raman bands at 882 and 993 cm^{-1} for detection can be collected from 850 to 1010 cm^{-1} (bluish rectangle-marked range in Fig. 5a) rather than scanning the whole Raman spectra. In addition, there is a linear relationship between the ratiometric peak intensity of I_{882}/I_{993} and the logarithmic concentrations of $ONOO^-$ over the range from 0.5 μM to 100 μM. Based on a signal-to-noise ratio of 3 (3 S/N), the limit of detection (LOD) can be calculated to be 0.4 μM. Therefore, the wide detection range and high sensitivity of the nanoprobe are suitable for the detection of $ONOO^-$ in living cells, especially under conditions of oxidative stress.

SERS imaging of the endogenous $ONOO^-$ in living cells

In living cells, $ONOO^-$ is generally synthesized by the reaction between nitric oxide (NO) and superoxide anion ($O_2^{\bullet-}$) which can be produced from L-arginine by nitric oxide synthetase and from O_2 by xanthine oxidase, respectively [30, 31]. Furthermore, high level of $ONOO^-$ is usually found in pathological process of tumor, and the endogenous generation of $ONOO^-$ can be promoted under stimulation of LPS, IFN-γ and PMA [32, 33]. To explore the biological application of the SERS nanoprobe, the cytotoxicity of RAW 264.7 macrophages by nanoprobe was firstly evaluated with 3-(4,5-dimethylthiazol-2-yl)-2,5-diphenyltetrazoliumbromide (MTT) assay. As shown in Fig. S9, the cell viability after 24 h of incubation is over 88%, which demonstrates that the nanoprobe has high biocompatibility and has enormous potential to apply in biological samples. Moreover, the dark-field image demonstrates that the AuNP/3-MPBAPE nanoprobes can distribute well in the cytoplasm of the tested cells after incubation for 2 h (Fig. S10).

In addition, RAW 264.7 macrophages were stimulated by LPS and IFN-γ for 12 h and PMA for 2 h to simulate an inflammatory situation to produce $ONOO^-$ endogenously [34]. And then SERS imaging were conducted according to the ratiometric peak intensity of I_{882}/I_{993} with the AuNP/3-MPBAPE probes loaded into cells sample. As Fig. 6 showed, with the concentrations of stimulators increasing, the colour of SERS imaging is gradually deeper and the area of signals becomes larger, which infers that the concentration of $ONOO^-$ is correspondingly rising. This result indicates that the SERS nanoprobe has a promising ability to detect and visualize the endogenous $ONOO^-$ in living cells. However, the quality of currently obtained SERS imaging is not perfect enough, which may be due to that SERS nanoprobes were not distributed uniformly in living cells. To acquire better SERS imaging, the intracellular dispersity of the nanoprobes needs to be further improved.

Conclusions

In summary, through assembling 3-MPBAPE molecules on AuNPs, $ONOO^-$ responsivity can be integrated with SERS activity into the AuNP/3-MPBAPE nanoprobe. Compared with the reported methods (Table S2), the SERS nanoprobe possesses comprehensive advantages in terms of response speed, sensitivity, linear range, and resistance of interference. This renders the SERS nanoprobe competent for the detection and imaging of the endogenous $ONOO^-$ in living cells. Although there is still scope to improve imaging quality by enhancing the intracellular dispersity of the nanoprobes, this SERS strategy shows a favorable potential in the researches of physiological process related with $ONOO^-$.

Acknowledgments The authors greatly appreciate the financial support from National Natural Science Foundation of China (21575041, 21777041), Shanghai Pujiang Program (17PJD010), and the Fundamental Research Funds for the Central Universities (222201718001, 222201717003).

Compliance with ethical standards The author(s) declare that they have no competing interests.

References

1. Finkel T, Holbrook NJ (2000) Oxidants, oxidative stress and the biology of ageing. Nature 408:239–247
2. Radi R (2013) Peroxynitrite, a stealthy biological oxidant. J Biol Chem 288:26464–26472
3. Ischiropoulos H, Beckman JS (2003) Oxidative stress and nitration in neurodegeneration: cause, effect, or association? J Clin Invest 111:163–169
4. Sarchielli P, Galli F, Floridi A, Floridi A, Gallai V (2003) Relevance of protein nitration in brain injury: a key pathophysiological mechanism in neurodegenerative, autoimmune, or inflammatory CNS diseases and stroke. Amino Acids 25:427–436
5. Wilcox CS, Pearlman A (2008) Chemistry and antihypertensive effects of tempol and other nitroxides. Pharmacol Rev 60:418–469
6. Sedgwick AC, Sun X, Kim G, Yoon J, Bull SD, James TD (2016) Boronate based fluorescence (ESIPT) probe for peroxynitrite. Chem Commun 52:12350–12352
7. Vasilescu A, Gheorghiu M, Peteu S (2017) Nanomaterial-based electrochemical sensors and optical probes for detection and imaging of peroxynitrite: a review. Microchim Acta 184:649–676
8. Hoebe RA, Van Oven CH, Gadella TWJ Jr, Dhonukshe PB, Van Noorden CJF, Manders EMM (2007) Controlled light-exposure microscopy reduces photobleaching and phototoxicity in fluorescence live-cell imaging. Nat Biotechnol 25:249–253
9. Pöhlker C, Huffman JA, Pöschl U (2012) Autofluorescence of atmospheric bioaerosols–fluorescent biomolecules and potential interferences. Atmos Meas Tech Discuss 5:37–71
10. Qu LL, Liu YY, He SH, Chen JQ, Liang Y, Li HT (2016) Highly selective and sensitive surface enhanced Raman scattering nanoprobes for detection of hydrogen peroxide in living cells. Biosens Bioelectron 7:292–298

11. Cortés E, Etchegoin PG, Le Ru EC, Fainstein A, Vela ME, Salvarezza RC (2010) Monitoring the electrochemistry of single molecules by surface-enhanced Raman spectroscopy. J Am Chem Soc 132:18034–18037
12. Li D, Qu L, Zhai W, Xue J, Fossey JS, Long Y (2011) Facile on-site detection of substituted aromatic pollutants in water using thin layer chromatography combined with surface-enhanced Raman spectroscopy. Environ Sci Technol 45:4046–4052
13. Vo-Dinh T (1995) SERS chemical sensors and biosensors: new tools for environmental and biological analysis. Sensors Actuators B Chem 29:183–189
14. Donnelly T, Smith WE, Faulds K, Graham D (2014) Silver and magnetic nanoparticles for sensitive DNA detection by SERS. Chem Commun 50:12907–12910
15. Xu LJ, Lei ZC, Li J, Zong C, Yang CJ, Ren B (2015) Label-free surface-enhanced Raman spectroscopy detection of DNA with single-base sensitivity. J Am Chem Soc 137:5149–5154
16. Guerrini L, Krpetić Ž, van Lierop D, Alvarez-Puebla RA, Graham D (2015) Direct surface-enhanced Raman scattering analysis of DNA duplexes. Angew Chem 127:1160–1164
17. Avella-Oliver M, Puchades R, Wachsmann-Hogiu S, Maquieira A (2017) Label-free SERS analysis of proteins and exosomes with large-scale substrates from recordable compact disks. Sensors Actuators B Chem 252:657–662
18. Alvarez-Puebla RA, Liz-Marzán LM (2012) SERS detection of small inorganic molecules and ions. Angew Chem Int Ed 51: 11214–11223
19. Cui J, Hu K, Sun JJ, Qu LL, Li DW (2016) SERS nanoprobes for the monitoring of endogenous nitric oxide in living cells. Biosens Bioelectron 85:324–330
20. Sun X, Xu Q, Kim G, Flower SE, Lowe JP, Yoon J, Fossey JS, Qian XH, Bull SD, James TD (2014) A water-soluble boronate-based fluorescent probe for the selective detection of peroxynitrite and imaging in living cells. Chem Sci 5:3368–3373
21. Lee PC, Meisel D (1982) Adsorption and surface-enhanced Raman of dyes on silver and gold sols. J Phys Chem 86:3391–3395
22. Chen ZJ, Ren W, Wright QE, Ai HW (2013) Genetically encoded fluorescent probe for the selective detection of peroxynitrite. J Am Chem Soc 135:14940–14943
23. Wang W, Zhang L, Li L, Tian Y (2016) A single nanoprobe for ratiometric imaging and biosensing of hypochlorite and glutathione in live cells using surface-enhanced raman scattering. Anal Chem 88:9518–9523
24. Sun ZN, Liu FQ, Chen Y, Tam PKH, Yang D (2008) A highly specific BODIPY-based fluorescent probe for the detection of hypochlorous acid. Org Lett 10:2171–2174
25. Xie W, Schlücker S (2018) Surface-enhanced Raman spectroscopic detection of molecular chemo-and plasmo-catalysis on noble metal nanoparticles. Chem Commun 54:2326–2336
26. Li DW, Qu LL, Hu K, Long YT, Tian H (2015) Monitoring of endogenous hydrogen sulfide in living cells using surface-enhanced Raman scattering. Angew Chem Int Ed 54:12758–12761
27. Sikora A, Zielonka J, Lopez M, Joseph J, Kalyanaraman B (2009) Direct oxidation of boronates by peroxynitrite: mechanism and implications in fluorescence imaging of peroxynitrite. Free Radic Biol Med 47:1401–1407
28. Cheng T, Jiao Z, Liu X, Zhang H (2018) Selective, fast and semi-automatic enrichment of nucleosides by using a phenylboronic acid modified hybrid material composed of graphene oxide and melamine sponge. Microchim Acta 185:348–353
29. Devi JA, Anulekshmi AH, Salini S, Aparna RS, George S (2017) Boronic acid functionalized nitrogen doped carbon dots for fluorescent turn-on detection of dopamine. Microchim Acta 184:4081–4090
30. Beckman JS, Beckman TW, Chen J, Marshall PA, Freeman BA (1990) Apparent hydroxyl radical production by peroxynitrite: implications for endothelial injury from nitric oxide and superoxide. Proc Natl Acad Sci USA 87:1620–1624
31. Ferrer-Sueta G, Campolo N, Trujillo M, Bartesaghi S, Carballal S, Romero N, Alvarez B, Radi R (2018) Biochemistry of peroxynitrite and protein tyrosine nitration. Chem Rev 118:1338–1408
32. Amatore C, Arbault S, Koh ACW (2010) Simultaneous detection of reactive oxygen and nitrogen species released by a single macrophage by triple potential-step chronoamperometry. Anal Chem 82: 1411–1419
33. Hashioka S, Han YH, Fujii S, Kato T, Monji A, Utsumi H, Sawadad M, Nakanishi H, Kanba S (2007) Phospholipids modulate superoxide and nitric oxide production by lipopolysaccharide and phorbol 12-myristate-13-acetate-activated microglia. Neurochem Int 50:499–506
34. Amatore C, Arbault S, Bouton C, Drapier JC, Ghandour H, Koh AC (2008) Real-time Amperometric analysis of reactive oxygen and nitrogen species released by single Immunostimulated macrophages. ChemBioChem 9:1472–1480